

lution, so it seems that these approaches are complementary to each other at least for $\pi/2$ pulse shaping. It would be illuminating to compare the numerical results from these two approaches. Work along this line is under way.

Acknowledgment. This work was supported by a 1994 institutional research fund from Sunmoon University.

References

1. For recent reviews see, (a) Shore, B. W. *Theory of Coherent Atomic Excitation*; Wiley: New York, U. S. A., 1990; Vol. I, Chapter 5. (b) Warren, W. S.; Silver, M. S. In *Advan. Magn. Reson.* **1988**, *12*, 247.
2. (a) Zakharov, V. E.; Shabat, A. B. *Sov. Phys.--JETP* **1972**, *34*, 62. (b) *Func. Anal. Appl.* **1974**, *8*, 226.
3. (a) Ablowitz, M. J.; Kaup, D. J.; Newell, A. C.; Segur, H. *Phys. Rev. Lett.* **1973**, *30*, 1262. (b) *ibid.* **1973**, *31*, 125. (c) *Stud. Appl. Math.* **1974**, *53*, 249.
4. An extensive list of evolution equations solvable by IS transform can be found in Calogero, F.; Degasperis, A. *Spectral Transform and Solitons I*; North-Holland: Amsterdam, Netherland, 1982.
5. For a general overview the reader is referred to Ghosh Roy, D. N. *Methods of Inverse Problems in Physics*; CRC Press: Boca Raton, U. S. A., 1991; Chapter 1.
6. (a) Grünbaum, A.; Hasenfeld, A. *Inverse Probl.* **1986**, *2*, 75. (b) *ibid.* **1988**, *4*, 485.
7. (a) Hasenfeld, A. *J. Mag. Res.* **1987**, *72*, 509. (b) Hasenfeld, A.; Hammes, S.; Warren, W. S. *Phys. Rev.* **1988**, *A38*, 2678.
8. (a) Lamb, Jr., G. L. *Rev. Mod. Phys.* **1971**, *43*, 99. (b) *Phys. Rev. Lett.* **1973**, *31*, 196. (c) *Elements of Soliton Theory*; Wiley: New York, U. S. A.; 1980.
9. Michalska-Trautman, R. *Phys. Rev.* **1981**, *A23*, 352. *ibid.* **1992**, *46*, 7270, and references therein.
10. The normalized bandwidth of a shaped pulse is defined as the ratio $\Delta\omega/\bar{\omega}$, where $\bar{\omega}$ is the root-mean-square pulse amplitude. See, for example, Zax, D. B.; Vega S. *Phys. Rev. Lett.* **1989**, *62*, 1840.
11. (a) Bargmann, V. *Rev. Mod. Phys.* **1949**, *21*, 488. (b) Landau, L. D.; Lifshitz, E. M. *Quantum Mechanics*; 3rd ed.; Pergamon: Oxford U. P., U. K.; 1977.
12. (a) McCall, S. L.; Hahn, E. L. *Phys. Rev. Lett.* **1967**, *18*, 908. (b) *Phys. Rev.* **1969**, *183*, 459.
13. Haus, H. *Rev. Mod. Phys.* **1979**, *51*, 331.
14. Lee, C. J. *Nuovo Cimento* **1993**, *108B*, 1299.
15. Buck, U. *Rev. Mod. Phys.* **1974**, *46*, 369.
16. Messiah, A. *Quantum Mechanics*; Vol. I; North-Holland: Amsterdam, Netherland; 1961.
17. A well-known example, in which a square of the δ -function appears in the intermediate step, is the calculation of the transition probability by time-dependent perturbation theory.

Theoretical Studies of Surface Diffusion: Multidimensional TST and Effect of Surface Vibrations

Kijeong Kwac, Seokmin Shin, Sangyoub Lee*, and Kook Joe Shin*

Department of Chemistry and Center for Molecular Catalysis, Seoul National University, Seoul 151, Korea

Received October 26, 1995

We present a theoretical formulation of diffusion process on solid surface based on multidimensional transition state theory (TST). Surface diffusion of single adatom results from hopping processes on corrugated potential surface and is affected by surface vibrations of surface atoms. The rate of rare events such as hopping between lattice sites can be calculated by transition state theory. In order to include the interactions of the adatom with surface vibrations, it is assumed that the coordinates of adatom are coupled to the bath of harmonic oscillators whose frequencies are those of surface phonon modes. When nearest neighbor surface atoms are considered, we can construct Hamiltonians which contain terms for interactions of adatom with surface vibrations for the well minimum and the saddle point configurations, respectively. The escape rate constants, thus the surface diffusion parameters, are obtained by normal mode analysis of the force constant matrix based on the Hamiltonian. The analysis is applied to the diffusion coefficients of W, Ir, Pt and Ta atoms on the bcc(110) plane of W in the zero-coverage limit. The results of the calculations are encouraging considering the limitations of the model considered in the study.

Introduction

Diffusion of atoms and molecules adsorbed on solid surfaces is an important and interesting phenomena both from a conceptual and a practical points of view.^{1,2} It is the primary mechanism of mass transport on solid surfaces. Surface diffusion plays a key role in the growth of thin films, the formation of epitaxial layers, and the catalytic reaction occurring

on metal surfaces.

The migration of adsorbed atoms on solid surfaces have been studied extensively both experimentally and theoretically. In recent years, the development of the field ion microscope (FIM) allows one to image the metal substrate surface in atomic resolution.^{1,4-6} Several elementary atomic processes on surface have been studied in detail with FIM: surface diffusion of single adatoms and small clusters, adatom-ada-

tom interactions, site-specific atom-substrate interactions, and adatom-lattice interactions. One can directly observe random walks of single adatoms and measure diffusion coefficients quantitatively. In molecular dynamics simulations of surface diffusion,⁷⁻¹³ one can follow the motions of individual atoms in detail, thus providing a test for approximate dynamical theories. Diffusion coefficients and activation energies can be easily calculated in the simulations. Several versions of transition state theory and quantum correlation function theory have also been used to study the mobility of heavy or light atoms.¹⁴⁻¹⁹

Experimental results indicate that the character of surface diffusion, in particular the diffusion mechanism, can vary depending on the substrate and the orientation of the surface. For example, simple hopping between adjacent sites often gives ways to adatom-substrate exchange.¹² In the case of diffusion on relatively smooth surfaces such as bcc(110) or fcc(110), it may be safe to assume that diffusion occurs via jumps from one adsorption site to another. In the present study, we theoretically investigate the diffusion of a single metal atom on the bcc(110) surface of a tungsten(W) substrate. We assume that the motion of the adatom consists of independent, randomly oriented, hops between adjacent binding sites. The motion obeys the random-walk statistics and the diffusion constant is given by¹⁵

$$D = \frac{l^2}{2d} k_{hop} \quad (1)$$

where l is the distance between binding sites, d is the dimensionality of the diffusional motion and k_{hop} is the rate of independent hops. In the simple transition state theory (TST), k_{hop} is represented as¹⁵

$$k_{hop} = n_p k_{TST}, \quad (2a)$$

$$k_{TST} = \nu \exp(-E_b/k_B T). \quad (2b)$$

where ν is the prefactor in the Arrhenius form of TST rate, E_b is the difference between the energies at the saddle point where the transition state is formed and at the well minimum on the potential energy surface. n_p is the number of binding sites accessible for a single hop and $k_B T$ is the Boltzmann factor. The calculation of TST rate is based on the assumption that no recrossings or multiple jumps occur and the adatom makes randomly oriented single jumps. It is also assumed that the escape frequency ν is independent of temperature. The Arrhenius parameters for the diffusion constant are given by

$$D = D_0 \exp(-E_b/k_B T), \quad (3a)$$

$$D_0 = \frac{n_p \nu l^2}{2d}, \quad (3b)$$

$$E_b = E(\text{saddle point}) - E(\text{well minimum}). \quad (3c)$$

We will show that the Arrhenius parameters for surface diffusion coefficient can be obtained by using multidimensional transition state theory.

Surface diffusion of single adatom results from hopping processes on the corrugated potential surface and its random-walk-like motion is affected by the surface vibrations of lattice atoms. It is necessary to include the coupling of adatom motion to surface phonon modes for the evaluation

of surface diffusion parameters. The change of surface phonon modes by the introduction of an adsorbed atom is ignored. The frequencies of phonon modes are calculated by treating the surface vibration in the limit of classical mechanics. The purpose of the present study is to calculate the diffusion parameters from the jump rate by using multidimensional TST^{20,22} based on the Hamiltonian constructed to include the terms for the interaction of adatom and surface vibration modes.

The remainder of the paper is organized as follows. Brief reviews of theoretical backgrounds for multidimensional TST and lattice dynamics are presented in the following section. In the third section, the evaluation of the escape(jump) rate is explained in terms of (i) method of determining well minimum and saddle point; (ii) Hamiltonian constructions appropriate for two configurations; (iii) rate constant expression. Results of model calculations for several metal atoms on W surface are given in the last section with some discussions.

Theoretical Backgrounds

Multidimensional TST. We consider a metastable system consisting of a reaction coordinate coupled to vibrational degrees of freedom. In TST, the reactant, product and saddle point geometries at which the gradient of potential energy vanishes are first located. The TST rate is given in terms of the product of all stable mode frequencies at the minimum and the inverse product of stable mode frequencies at the saddle point, respectively.^{20,21}

$$k_{TST} = \frac{1}{2\pi} \frac{\prod_{i=0}^{\gamma} \lambda_i^{(a)}}{\prod_{i=0}^{\gamma} \lambda_i^{(b)}} \exp(-\beta E_b) \quad (4)$$

where λ 's are normal modes eigenvalues $\{(\lambda_i^{(a)})^2 > 0, i=0, \dots, \gamma\}$, $\{-(\lambda_0^{(b)})^2 < 0, (\lambda_i^{(b)})^2 > 0, i=1, \dots, \gamma\}$, obtained from the force constant matrices, and γ is the number of the coupled harmonic oscillators.

As a model case, we consider a particle of mass M , whose coordinates x is coupled bilinearly to the bath of harmonic oscillators. The total Hamiltonian H of the system and bath is then of the form^{22,23}

$$H = \frac{p^2}{2M} + U(x) + \frac{1}{2} \sum_{i=1}^r m_i \left[\dot{q}_i^2 + \omega_i^2 \left(q + \frac{C_i}{m_i \omega_i} x \right)^2 \right] \quad (5)$$

Here bath is composed of harmonic oscillators with mass $\{m_i\}$ and frequencies $\{\omega_i\}$ and C_i 's are constants for coupling.

The normal mode eigenvalues entering the transition state rate may be evaluated *via* a normal mode analysis of the full Hamiltonian at the saddle point and at the well minimum. The potential $U(x)$ is approximated at the well minimum as $U(x) \cong (1/2) M \omega_0^2 (x + x_0)^2$, $x_0 > 0$, and at the barrier by $U(x) \cong E_b - (1/2) M \omega_b^2 x^2$. The total Hamiltonian may be written in the vicinity of the well minimum and the barrier in a separate form as a sum of $(\gamma + 1)$ harmonic oscillators.

Using standard techniques, we first transform to mass-weighted coordinates and then diagonalize the $(\gamma + 1)$ by $(\gamma + 1)$ force constant matrix K . If we denote the second derivative matrices at the saddle point and at the well bottom as $K^{(b)}$ and $K^{(a)}$, respectively, one can prove the following identities for the determinants of $K^{(b)}$ and $K^{(a)}$.^{22,23}

Table 1. The Morse potential parameters²⁵

Material	U_0 (eV)	ξ (Å)	d (Å)
W	0.9710	1.3850	3.053 (3.253*)
Pt	0.7102	1.6047	2.897
Ir	0.8435	1.6260	2.864
Ta	0.7504	1.1319	3.346

*This value is used for the calculation of the phonon frequency of the substrate surface.

$$\det(K^{(b)}) = -(\lambda_0^{(b)})^2 \prod_{i=1}^Y (\lambda_i^{(b)})^2 = -\omega_b^2 \prod_{i=1}^Y \omega_i^2 \quad (6a)$$

$$\det(K^{(o)}) = (\lambda_0^{(o)})^2 \prod_{i=1}^Y (\lambda_i^{(o)})^2 = \omega_o^2 \prod_{i=1}^Y \omega_i^2 \quad (6b)$$

then we can recast Eq. (4) as^{22,23}

$$k_{TST} = \frac{\lambda_0^{(b)}}{\omega_b} \frac{\omega_0}{2\pi} \exp(-\beta E_b) \quad (7)$$

which is just the result obtained by Grote and Hynes.²⁴ Considering the average motion of the particle in the vicinity of the barrier, Grote and Hynes found that on the average the particle is not moving on the bare barrier whose imaginary frequency is ω_b but rather on an effective barrier whose imaginary frequency is $\lambda_0^{(b)}$. Pollak²² modeled the generalized Langevin equation (GLE) via a harmonic bath by using the Hamiltonian of the form as in Eq. (5) to show that the reactive frequency $\lambda_0^{(b)}$ is exactly an imaginary frequency of a barrier that has been modified by the bath.

On the application of the above formalism, the motion of adatom on the surface can be regarded as the motion of a particle coupled to the bath of harmonic oscillators whose frequencies are those of surface phonon modes. The change we impose on the above formalism is that the particle coupled to the harmonic oscillators can move in three-dimensional space instead of one-dimensional coordinates. Then, what we are to obtain is an Hamiltonian expression which contain the coupling coefficient C_i 's calculated explicitly. From that Hamiltonian we obtain $\lambda_0^{(b)}$ through a normal mode analysis and calculate the hopping rate.

Lattice Dynamics. The bcc(110) surface of tungsten is chosen for the calculation. Only the first layer of surface is considered and the effects of second layer and below are ignored. The number of surface atoms included in the calculation is $11 \times 11 = 121$.

Interaction potential between the surface atoms is assumed to be a pairwise additive Morse potential:

$$V_{ij} = U_0 \{ \exp[-2\xi(r_{ij} - d)] - 2\exp[-\xi(r_{ij} - d)] \} \quad (8)$$

where r_{ij} is the distance between atom i and atom j and U_0 , ξ , d are constants characteristic of the pair of atoms. The interaction between the adatom and the surface atom is also assumed to be a pairwise additive Morse potential. The parameters U_0 , ξ , and d are determined based on the bulk lattice constant, cohesive energy, and compressibility. The values used in this study are shown²⁵ in Table 1. For two atoms of different kinds, we use the value which is arithmetic mean of corresponding two parameter values.

We briefly review parts of the theory of lattice dynamics²⁶⁻²⁸

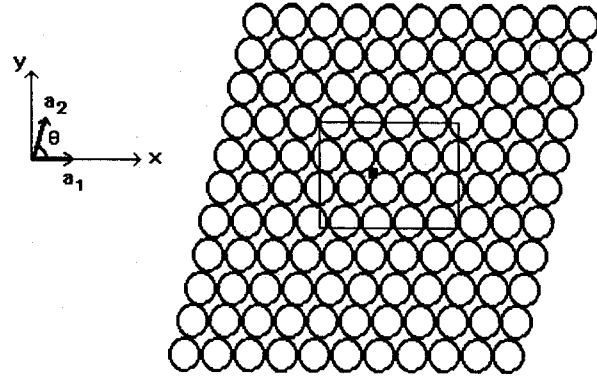


Figure 1. bcc(110) surface considered in the present study. A small shaded square (■) indicates the binding site minimum and the area enclosed by a rectangle is viewed in Figures 2. and 3.

used in this work. In the absence of adatoms, the mean positions of atoms of a surface are arranged in a regular array. The lattice site is specified by primitive basic lattice translation vectors \mathbf{a}_1 , \mathbf{a}_2 as shown in Fig. 1. The index of lattice atom is (n_1, n_2) , which we will refer to collectively as \mathbf{n} . We denote the equilibrium position vector of the lattice atom in the simple lattice by $\mathbf{l}_n = n_1\mathbf{a}_1 + n_2\mathbf{a}_2$.

The interatomic potential is assumed to be central force potential, depending only on the magnitude of the separation between atoms. Then the total potential energy W of clean surface is of the form:

$$W = \frac{1}{2} \sum_n \sum_{m(\neq n)} \phi(r_{nm}) \quad (9)$$

where $r_{nm} = (l_{nm}^2 + 2\mathbf{l}_{nm} \cdot \mathbf{u}_{nm} + u_{nm}^2)^{1/2}$, $\mathbf{l}_{nm} = \mathbf{l}_n - \mathbf{l}_m$, and $\mathbf{u}_{nm} = \mathbf{u}_n - \mathbf{u}_m$. Here \mathbf{l}_n is lattice translation vector and \mathbf{u}_n is displacement vector from its equilibrium position. In this work the central force potential $\phi(r)$ is the Morse potential of the form as in Eq. (8).

The total potential energy W of the surface is assumed to be some function of the instantaneous positions of all atoms. In the harmonic approximation with respect to the atomic displacements, W is expanded as follows:

$$W = W_0 + \frac{1}{2} \sum_{n, \alpha} \sum_{m, \beta} W_{\alpha\beta}(n; m) u_\alpha(n) u_\beta(m) \quad (10)$$

with

$$W_{\alpha\beta}(n; m) = \left. \frac{\delta^2 W}{\delta u_\alpha(n) \delta u_\beta(m)} \right|_0 \quad (11)$$

where α and β refer to x or y , and subscript 0 means evaluation at $\mathbf{u} = 0$. If we recast the expansion coefficients in terms of pairwise potential,²⁶

$$W_{\alpha\beta}(n; m) = -\Phi_{\alpha\beta}(n; m), \quad n \neq m, \quad (12a)$$

$$W_{\alpha\beta}(n; n) = \sum_{m(\neq n)} \Phi_{\alpha\beta}(n; m) \quad (12b)$$

where

$$\Phi_{\alpha\alpha}(n; m) = \left\{ \frac{l_\alpha^2}{r^2} \left[\phi''(r) - \frac{1}{r} \phi'(r) \right] + \frac{1}{r} \phi'(r) \right\} \Big|_{r=l_{nm}} \quad (13a)$$

$$\Phi_{\alpha\beta}(n;m) = \left\{ \frac{I_{\beta}^{\alpha}}{r^2} \left[\phi''(r) - \frac{1}{r} \phi'(r) \right] \right\}_{r=l_{nm}} \quad (13b)$$

We introduce the Fourier transform of the reduced displacement $w(n) = \sqrt{M} u(n)$ as

$$w_{\alpha}(n) = \frac{1}{\sqrt{N}} \sum_{\mathbf{k}} f_{\alpha}(\mathbf{k}) \exp(i\mathbf{k} \cdot \mathbf{l}_n) \quad (14)$$

Then we can represent the dynamical matrix, which is real and symmetric, as

$$\begin{aligned} D_{\alpha\beta}(\mathbf{k}) &= \frac{1}{M} \sum_m W_{\alpha\beta}(0;m) \exp(i\mathbf{k} \cdot \mathbf{l}_m) \\ &= \frac{1}{M} \left\{ \sum_{m(\neq 0)} \Phi_{\alpha\beta}(0;m) - \sum_{m(\neq 0)} \Phi_{\alpha\beta}(0;m) \cos(\mathbf{k} \cdot \mathbf{l}_m) \right\} \quad (15) \end{aligned}$$

From this matrix we can calculate eigenvalues, $\omega_1^2(\mathbf{k})$, $\omega_2^2(\mathbf{k})$ and corresponding eigenvectors, $(e_x^1(\mathbf{k}), e_y^1(\mathbf{k}))$, $(e_x^2(\mathbf{k}), e_y^2(\mathbf{k}))$, which satisfy the orthogonality and closure conditions

$$\sum_{\alpha} e_{\alpha}^s(\mathbf{k}) e_{\alpha}^{s'}(\mathbf{k}) = \delta_{ss'}, \quad \sum_s e_{\alpha}^s(\mathbf{k}) e_{\beta}^s(\mathbf{k}) = \delta_{\alpha\beta} \quad (16)$$

From the normal coordinates, $Q_s(\mathbf{k})$, defined as

$$f_{\alpha}(\mathbf{k}) = e_{\alpha}^1(\mathbf{k}) Q_1(\mathbf{k}) + e_{\alpha}^2(\mathbf{k}) Q_2(\mathbf{k}) \quad (17)$$

we obtain the real normal coordinates as follows:

$$Z_1^s(\mathbf{k}) = \frac{1}{\sqrt{2}} [Q_s(\mathbf{k}) + Q_s^*(\mathbf{k})] = \frac{1}{\sqrt{2}} [Q_s(\mathbf{k}) + Q_s(-\mathbf{k})] \quad (18a)$$

$$Z_2^s(\mathbf{k}) = \frac{1}{\sqrt{2}} [Q_s(\mathbf{k}) - Q_s^*(\mathbf{k})] = \frac{1}{\sqrt{2}} [Q_s(\mathbf{k}) - Q_s(-\mathbf{k})] \quad (18b)$$

The Hamiltonian for the clean lattice is then given by

$$H = \frac{1}{2} \sum_{\mathbf{k}>0} \sum_{rs} [\dot{Z}_r^s(\mathbf{k})]^2 + \frac{1}{2} \sum_{\mathbf{k}>0} \sum_{rs} \omega_s^2(\mathbf{k}) [Z_r^s(\mathbf{k})]^2 \quad (19)$$

where $\mathbf{k}>0$ signifies that \mathbf{k} is summed over the permitted wave numbers lying on one side of the line through the origin of the reciprocal lattice plane.

Any displacement of lattice atom can be represented as linear combinations of surface vibration modes:

$$\begin{aligned} u_{\alpha}(n) &= \sqrt{\frac{2}{MN}} \sum_{\mathbf{k}>0} [e_{\alpha}^1(\mathbf{k}) \{Z_1^1(\mathbf{k}) \cos(\mathbf{k} \cdot \mathbf{l}_n) - Z_2^1(\mathbf{k}) \sin(\mathbf{k} \cdot \mathbf{l}_n)\} \\ &\quad + e_{\alpha}^2(\mathbf{k}) \{Z_1^2(\mathbf{k}) \cos(\mathbf{k} \cdot \mathbf{l}_n) - Z_2^2(\mathbf{k}) \sin(\mathbf{k} \cdot \mathbf{l}_n)\}] \quad (20) \end{aligned}$$

Therefore the interaction energy expression between adatom and surface vibrations can be constructed from the atomic displacements, $u(n)$.

Escape Rate

Well minimum and Saddle Point. We consider a single adatom adsorbed in the clean surface. For implementing TST, we need to define the reaction (diffusion) pathway and identify the transition state. Even for single atom diffusion we must consider the behavior of the neighboring substrate atoms in addition to the adatom itself. It is the configuration of all atomic positions which defines the well minimum and the saddle point positions on potential energy surface. One should consider the interactions between adatom and all the atoms on the surface in order to determine the well mini-

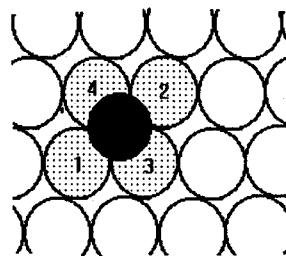


Figure 2. The well minimum configuration of an adatom on the bcc(110) surface. Four atoms indexed 1, 2, 3, 4 are permitted to relax.

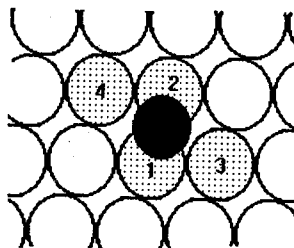


Figure 3. The saddle point configuration of an adatom on the bcc(110) surface. Four atoms indexed 1, 2, 3, 4 are permitted to relax.

mum and TS configurations.

As an approximation, only four nearest neighbor surface atoms of adatom are permitted to relax and all the other atoms are fixed at their lattice sites. The four atoms permitted to move for the determination of well minimum configuration are different from those for the saddle point configuration. The two cases are shown in Figures 2 and 3. As indicated in the figures, only atoms numbered 1 to 4 can move. The remainder of surface atoms are numbered from 5 to 121.

From symmetry, the adatom position corresponding to the well minimum is the four-fold site and the saddle point is halfway between two adjacent four-fold sites. So only the z -coordinate of the adatom is to be determined. In determining the position of adatom and the displacements of four surface atoms in the neighborhood, we consider the following potential function V_p :

$$V_p = \sum_{i=1}^N U_o' \{ \exp[-2\xi'(x_i - d')] - 2 \exp[-\xi'(x_i - d)] \} + \sum_{j=1}^4 V_j^s \quad (21)$$

$$V_j^s = \sum_{i=j+1}^N U_o \{ \exp[-2\xi(y_i - d)] - 2 \exp[-\xi(y_i - d)] \} \quad (22)$$

where U_o' , ξ' , d' are parameters for the interactions between the adatom and a surface atom, while U_o , ξ , d are those between two surface atoms. $x_i = |\mathbf{q} - \mathbf{r}_i|$ refers to the distance between the adatom and surface atoms and $y_i = |\mathbf{r}_j - \mathbf{r}_i|$ to that between the movable surface atom and the other surface atoms. Then V_p is a function of nine variables: z -coordinate of the adatom and the displacements of four neighboring surface atoms. One can find the values of these variables which minimize the V_p in the saddle point region and well minimum region separately. The activation energy for escape,

Table 2. The Arrhenius parameters

Adatom/Surface	Theoretical	Experimental [ref.]
W/W(110)		
D_0 (cm ² /s)	4.175×10^{-4}	2.1×10^{-3} [4]
E_b (kJ/mol)	51.51	83.26 [4]
Pt/W(110)		
D_0 (cm ² /s)	3.539×10^{-4}	3×10^{-3} [6]
E_b (kJ/mol)	50.36	65 [6]
Ir/W(110)		
D_0 (cm ² /s)	5.543×10^{-4}	1×10^{-5} [5]
E_b (kJ/mol)	54.31	67.6 [5]
Ta/W(110)		
D_0 (cm ² /s)	4.206×10^{-4}	4×10^{-2} [4]
E_b (kJ/mol)	40.90	75 [4]

E_b is obtained as the difference of interaction potentials at two configurations:

$$E_b = V_p \text{ (at the saddle point)} - V_p \text{ (at the well minimum)} \quad (23)$$

For the cases of the four adatoms, W, Pt, Ir, Ta, on the surface of W(110), the calculated values of E_b are given in Table 2.

Hamiltonian Expression. Hamiltonian expressions near the well minimum and the saddle point can be constructed from the configurations determined as in the preceding section. We first consider the saddle point configuration. The coordinate of the adatom can be expressed as

$$\mathbf{q} = \left(\frac{a}{2} \cos\theta + q_x, \frac{a}{2} \sin\theta + q_y, b_s + q_z \right) \quad (24)$$

where b_s is the z-coordinate of adatom at the saddle point and q_x, q_y, q_z are displacements from the saddle point configuration.

The interaction between single adatom and lattice atoms of the surface is given by Eq. (21). As an approximation, we fix all the surface atoms at their lattice sites except four nearest neighbor surface atoms of 1 to 4 around the adatom. Then we can write the interaction potential in terms of the displacements of the adatom and the four surface atoms. The Hamiltonian which is valid near the saddle point consists of the following terms:

$$H = H_s + H_a + H_c \quad (25)$$

where H_s is the Hamiltonian for the surface atoms, H_a is the Hamiltonian for the adsorbed atom and H_c represents the coupling between the adatom and the surface atoms. We take the Hamiltonian expression of clean two-dimensional lattice, Eq. (19), for H_s . The expressions of H_a and H_c can be written by using the potential energy expression for the interaction between adatom and surface atoms obtained as above.

We use M to denote the mass of adatom and m the mass of surface atom respectively and introduce the mass-weighted coordinates of adatom, $g = \sqrt{M}q$. We also substitute the linear combinations of surface phonon modes, $Z_1^1(\mathbf{k}), Z_1^2(\mathbf{k}), Z_2^1(\mathbf{k}), Z_2^2(\mathbf{k})$ for the surface atom displacements as in Eq. (20). Then, the total Hamiltonian can be recast as follows:

$$\begin{aligned}
 H = & \frac{1}{2} \sum_{\mathbf{k}>0} \sum_{r,s} [\dot{Z}_r^s(\mathbf{k})]^2 + \frac{1}{2} \sum_{\mathbf{k}>0} \sum_{r,s} \omega_s^2(\mathbf{k}) [Z_r^s(\mathbf{k})]^2 + \frac{1}{2} (\dot{q}_x^2 + \dot{q}_y^2 + \dot{q}_z^2) \\
 & + V(b) \\
 & + \frac{1}{2M} A_{xx} g_x^2 + \frac{1}{2M} A_{yy} g_y^2 + \frac{1}{2M} A_{zz} g_z^2 + \frac{1}{M} A_{xy} g_x g_y \\
 & + \frac{1}{M} A_{yz} g_y g_z + \frac{1}{M} A_{zx} g_z g_x \\
 & + \sqrt{\frac{2}{mMN}} \sum_{s=1,2} \sum_{\mathbf{k}>0} \left\{ e_x^s(\mathbf{k}) \sum_{i=1}^4 C_{xix} \cos(\mathbf{k} \cdot \mathbf{l}_i) \right. \\
 & \left. + e_y^s(\mathbf{k}) \sum_{i=1}^4 C_{xiy} \cos(\mathbf{k} \cdot \mathbf{l}_i) \right\} Z_1^s(\mathbf{k}) g_x \\
 & - \sqrt{\frac{2}{mMN}} \sum_{s=1,2} \sum_{\mathbf{k}>0} \left\{ e_x^s(\mathbf{k}) \sum_{i=1}^4 C_{xix} \sin(\mathbf{k} \cdot \mathbf{l}_i) \right. \\
 & \left. + e_y^s(\mathbf{k}) \sum_{i=1}^4 C_{xiy} \sin(\mathbf{k} \cdot \mathbf{l}_i) \right\} Z_2^s(\mathbf{k}) g_x \\
 & + \sqrt{\frac{2}{mMN}} \sum_{s=1,2} \sum_{\mathbf{k}>0} \left\{ e_x^s(\mathbf{k}) \sum_{i=1}^4 C_{yix} \cos(\mathbf{k} \cdot \mathbf{l}_i) \right. \\
 & \left. + e_y^s(\mathbf{k}) \sum_{i=1}^4 C_{yiy} \cos(\mathbf{k} \cdot \mathbf{l}_i) \right\} Z_1^s(\mathbf{k}) g_y \\
 & - \sqrt{\frac{2}{mMN}} \sum_{s=1,2} \sum_{\mathbf{k}>0} \left\{ e_x^s(\mathbf{k}) \sum_{i=1}^4 C_{yix} \sin(\mathbf{k} \cdot \mathbf{l}_i) \right. \\
 & \left. + e_y^s(\mathbf{k}) \sum_{i=1}^4 C_{yiy} \sin(\mathbf{k} \cdot \mathbf{l}_i) \right\} Z_2^s(\mathbf{k}) g_y \\
 & + \sqrt{\frac{2}{mMN}} \sum_{s=1,2} \sum_{\mathbf{k}>0} \left\{ e_x^s(\mathbf{k}) \sum_{i=1}^4 C_{zix} \cos(\mathbf{k} \cdot \mathbf{l}_i) \right. \\
 & \left. + e_y^s(\mathbf{k}) \sum_{i=1}^4 C_{ziy} \cos(\mathbf{k} \cdot \mathbf{l}_i) \right\} Z_1^s(\mathbf{k}) g_z \\
 & - \sqrt{\frac{2}{mMN}} \sum_{s=1,2} \sum_{\mathbf{k}>0} \left\{ e_x^s(\mathbf{k}) \sum_{i=1}^4 C_{zix} \sin(\mathbf{k} \cdot \mathbf{l}_i) \right. \\
 & \left. + e_y^s(\mathbf{k}) \sum_{i=1}^4 C_{ziy} \sin(\mathbf{k} \cdot \mathbf{l}_i) \right\} Z_2^s(\mathbf{k}) g_z \quad (26)
 \end{aligned}$$

where

$$A_{xx} = \frac{\delta^2 V}{\delta q_x^2} \Big|_0, \quad A_{xy} = \frac{\delta^2 V}{\delta q_x \delta q_y} \Big|_0, \dots, \quad (27a)$$

$$C_{xix} = \frac{\delta^2 V}{\delta q_x \delta u_{ix}} \Big|_0, \quad C_{xiy} = \frac{\delta^2 V}{\delta q_x \delta q_{iy}} \Big|_0, \dots, \quad (27b)$$

with the subscript 0 meaning the evaluation at the saddle point configuration.

From this Hamiltonian expression at the saddle point, we can make the $[3+2(N-1)] \times [3+2(N-1)]$ force constant matrix, $K^{(b)}$, whose elements are second derivatives of the total potential energy evaluated at the saddle point. Diagonalizing the force constant matrix, $K^{(b)}$, we can obtain the eigenvalues, $\{-(\lambda_0^{(b)})^2 < 0, (\lambda_i^{(b)})^2 > 0, i=1, \dots, 2N+1\}$. The relation for the determinant corresponding to Eq. (6a) is

$$\begin{aligned}
 \det(K^{(b)}) &= -(\lambda_0^{(b)})^2 \prod_{i=1}^{2N} (\lambda_i^{(b)})^2 \\
 &= \mathbf{M}_b \prod_{\mathbf{k}>0} \omega_1^2(\mathbf{k}) \omega_1^2(\mathbf{k}) \omega_2^2(\mathbf{k}) \omega_2^2(\mathbf{k}) \quad (28)
 \end{aligned}$$

with

$$\mathbf{M}_b = \begin{vmatrix} M_{xx} & M_{xy} & M_{xz} \\ M_{xy} & M_{yy} & M_{yz} \\ M_{xz} & M_{yz} & M_{zz} \end{vmatrix} \quad (29)$$

where values of elements, M_{pq} , are calculated in the course of eliminating the upper elements of symmetric matrix, $K^{(b)}$. Detailed expressions are given in the Appendix.

So far we have considered the normal mode analysis at the saddle point. Exactly the same procedure is repeated for the well minimum. In this case the coordinates of the adatom can be expressed as

$$q = \left(-\frac{a}{2} + \frac{a}{2} \cos\theta + q_x, \frac{a}{2} \sin\theta + q_y, b_w + q_z \right) \quad (30)$$

where b_w is the z-coordinate position of adatom at the well minimum and q_x, q_y, q_z are displacements from the well minimum configuration. Repeating the same procedure as before, we can obtain the Hamiltonian expression for the well minimum as in Eq. (26) with different coefficients. In this case the second derivatives are evaluated at the well minimum. From the Hamiltonian for the well minimum, we can obtain the force constant matrix, $K^{(o)}$, whose eigenvalues are $\{(\lambda_i^{(o)})^2 > 0, i=0, \dots, 2N+1\}$. The relation for the determinant corresponding to Eq. (6b) is

$$\det(K^{(o)}) = \prod_{i=0}^{2N} (\lambda_i^{(o)})^2 = M_w \prod_{k>0} \omega_1^2(k) \omega_1^2(k) \omega_2^2(k) \omega_2^2(k) \quad (31)$$

where M_w is 3 by 3 matrix which is obtained exactly the same procedure as M_b .

Rate Constant. If we substitute Eqs. (28) and (31) in Eq. (4), then the rate of escape is represented as follows:

$$k_{TST} = \frac{\lambda_0^{(b)}}{2\pi} \sqrt{\frac{M_w}{-M_b}} \exp(-E_b/k_B T) \quad (32)$$

By comparing Eq. (2) with Eq. (32), we can obtain the surface diffusion parameters.

Results

The calculated values are given in Table 2 together with corresponding experimental values obtained by FIM experiment.⁴⁻⁶ The calculated D_0 values are slightly less than 10^{-3} , which is the typical value of pre-exponential factor for the surface diffusion. When the size of surface is increased, the unstable mode frequency changes only slightly under the condition that the size of surface is not too small. When the size of the surface layer is increased from n by n to $(n+1)$ by $(n+1)$ for n larger than 6, the unstable mode frequency increased by the factor of 10^{-5} or 10^{-4} . In our calculation, D_0 and E_b are calculated independently in contrast to the experimental procedure. If we permit the more surface atoms to relax in the calculation of activation energy, then the more accurate values of E_b can be obtained. But our main focus in this work is on the prefactor, D_0 , of the Arrhenius form of rate expression, which represents the dynamical aspects of the process while the activation energy reflects the static feature.

Some of the discrepancies between calculated and experimental values may result from the effects of the atoms in the second layer which we ignored. It can be argued that the interaction of the adatom with the second layer atoms located just below the adatom is more effective than with the edge atoms of the first layer. The presence of the second layer or several layers below the first layer may also influ-

ence the vibrating motions of first layer atoms even in the cases where the atoms below the first layer are fixed. One can test these effects in the computer simulation studies.

We are primarily interested in the application of the formalism of the multidimensional TST using the Hamiltonian which involves the system-bath interactions. Our application is for the surface diffusion process on the solid surface. Contrasted to the motions of solvent molecules in liquid phase, the motions of the atoms of the solid surface are relatively in order. As shown in this work, it is possible to determine the coefficients of the coupling between the system and bath explicitly for the motion of adatom on the solid surface. In this aspect, Tsekov and Ruckenstein's work²⁹ has some related features to this work. They considered Hamiltonian containing the linear coupling between the adsorbate and the substrate. But the effect of the phonon mode on the motion of the adsorbate is treated through one parameter, Debye frequency, ω_D . We do not reduce the effect of the surface vibrations on the motion of the adsorbate to a few parameters. The characteristic feature of this work is that each vibration mode of the surface is considered in detail and the coefficient representing its interaction with the adsorbate is determined explicitly.

In the dynamic process considered here, the adsorbed atom is activated by the interaction with the surface vibration, crosses over a barrier to a nearest binding site, and then relaxes at that site. These series of motions are activated process and the barrier crossing step is a rare event. So our result is not applicable to the surface diffusion at high temperature. More meaningful comparison would be made with the molecular dynamics simulation results using the same potential function. The results of present calculations are encouraging considering that the parameters used in the Morse potential are derived from bulk thermodynamic data and only the first layer of the surface is included.

Acknowledgment. This work was supported by a grant (No. BSRI-92-311) from the Basic Science Research Program, Ministry of Education and by the Center for Molecular Catalysis of the Korea Science and Engineering Foundation.

Appendix

To calculate the determinant of the force constant matrix, we eliminate the (n, m) elements of the matrix ($1 \leq n \leq 3, m \geq 4$). If we multiply the m th row with $-A_{mn}/\omega_s^2(k)$ where A_{mn} is the element of m th row and n th column of the matrix ($A_{mn} = A_{nm}$), and add this product to the n th row, then we can eliminate the (n, m) element. Repeating this procedure for $1 \leq n \leq 3, m \geq 4$, then determinant M_b is obtained as Eq. (29) with M_{pq} as follows. Calculation of M_w is exactly the same.

$$\begin{aligned} M_{pq} &= \frac{A_{pq}}{M} \\ &- \frac{2}{mMN} \sum_{k>0} \frac{1}{\omega_1^2(k)} \left\{ e_x^1(k) \sum_{i=1}^4 C_{pix} \cos(k \cdot l_i) + e_y^1(k) \sum_{i=1}^4 C_{piy} \cos(k \cdot l_i) \right\} \\ &\times \left\{ e_x^1(k) \sum_{i=1}^4 C_{pix} \cos(k \cdot l_i) + e_y^1(k) \sum_{i=1}^4 C_{piy} \cos(k \cdot l_i) \right\} \\ &- \frac{2}{mMN} \sum_{k>0} \frac{1}{\omega_1^2(k)} \left\{ e_x^1(k) \sum_{i=1}^4 C_{pix} \sin(k \cdot l_i) + e_y^1(k) \sum_{i=1}^4 C_{piy} \sin(k \cdot l_i) \right\} \end{aligned}$$

$$\begin{aligned} & \times \left\{ e_x^1(\mathbf{k}) \sum_{i=1}^4 C_{pix} \sin(\mathbf{k} \cdot \mathbf{l}_i) + e_y^1(\mathbf{k}) \sum_{i=1}^4 C_{piy} \sin(\mathbf{k} \cdot \mathbf{l}_i) \right\} \\ & - \frac{2}{mMN} \sum_{\mathbf{k} > 0} \frac{1}{\omega_1^2(\mathbf{k})} \left\{ e_x^2(\mathbf{k}) \sum_{i=1}^4 C_{pix} \cos(\mathbf{k} \cdot \mathbf{l}_i) + e_y^2(\mathbf{k}) \sum_{i=1}^4 C_{piy} \cos(\mathbf{k} \cdot \mathbf{l}_i) \right\} \\ & \times \left\{ e_x^2(\mathbf{k}) \sum_{i=1}^4 C_{pix} \cos(\mathbf{k} \cdot \mathbf{l}_i) + e_y^2(\mathbf{k}) \sum_{i=1}^4 C_{piy} \cos(\mathbf{k} \cdot \mathbf{l}_i) \right\} \\ & - \frac{2}{mMN} \sum_{\mathbf{k} > 0} \frac{1}{\omega_1^2(\mathbf{k})} \left\{ e_x^2(\mathbf{k}) \sum_{i=1}^4 C_{pix} \sin(\mathbf{k} \cdot \mathbf{l}_i) + e_y^2(\mathbf{k}) \sum_{i=1}^4 C_{piy} \sin(\mathbf{k} \cdot \mathbf{l}_i) \right\} \\ & \times \left\{ e_x^2(\mathbf{k}) \sum_{i=1}^4 C_{pix} \sin(\mathbf{k} \cdot \mathbf{l}_i) + e_y^2(\mathbf{k}) \sum_{i=1}^4 C_{piy} \sin(\mathbf{k} \cdot \mathbf{l}_i) \right\} \end{aligned}$$

where $p=x, y, z$ and $q=x, y, z$.

References

- Ehrlich, G.; Stolt, K. *Ann. Rev. Phys. Chem.* **1980**, *31*, 603.
- Surface Mobilities on Solid Materials*; Binh, V. T., Ed.; Plenum: New York, 1983.
- Doll, J. D.; Voter, A. F. *Ann. Rev. Phys. Chem.* **1987**, *38*, 413.
- Bassett, D. W.; Parsley, M. J. *J. Phys.* **1970**, *D3*, 707.
- Tsong, T. T.; Kellogg, G. *Phys. Rev.* **1975**, *B12*, 1343.
- Bassett, D. W. *J. Phys.* **1976**, *C9*, 2491.
- Tully, J. C.; Gilmer, H.; Shugard, M. *J. Chem. Phys.* **1979**, *71*, 1630.
- Mruzik, M. R.; Pound, G. M. *J. Phys.* **1981**, *F11*, 14 03.
- McDowell, H. K.; Doll, J. D. *Surf. Sci.* **1982**, *121*, L537.
- Doll, J. D.; Freeman, D. L. *Surf. Sci.* **1983**, *134*, 769.
- Voter, A. F.; Doll, J. D. *J. Chem. Phys.* **1985**, *82*, 80.
- Lynden-Bell, R. M. *Surf. Sci.* **1991**, *259*, 129.
- Park, S. C.; Bowman, J. M. *J. Chem. Phys.* **1984**, *80*, 2191.
- Jaquet, R.; Miller, W. H. *J. Phys. Chem.* **1985**, *89*, 2139.
- Voter, A. F.; Doll, J. D. *J. Chem. Phys.* **1984**, *80*, 5814, 5832.
- Truong, T. N.; Truhlar, D. G. *J. Phys. Chem.* **1987**, *91*, 6229.
- (a) Wahnstrom, G.; Haug, K.; Metiu, H. *Chem. Phys. Lett.* **1988**, *148*, 158. (b) Wahnstrom, G.; Haug, K.; Metiu, H. *J. Chem. Phys.* **1989**, *90*, 540.
- Rice, B. M.; Raff, L. M.; Thopson, D. L. *J. Chem. Phys.* **1988**, *88*, 7221.
- Rice, B. M.; Garrett, B. C.; Koszykowski, M. L.; Foiles, S. M.; Daw, M. S. *J. Chem. Phys.* **1990**, 775.
- Hanggi, P.; Talkner, P.; Borkovec, M. *Rev. Mod. Phys.* **1990**, *62*, 251.
- Slater, N. B. *Theory of Unimolecular Reactions*; Cornell U. P.: Ithaca, New York, 1959.
- Pollak, E. *J. Chem. Phys.* **1986**, *85*, 865.
- Pollak, E.; Grabert, H.; Hanggi, P. *J. Chem. Phys.* **1989**, *91*, 4073.
- Grote, R. F.; Hynes, J. T. *J. Chem. Phys.* **1980**, *73*, 2715.
- Flahive, P. G.; Graham, W. R. *Surf. Sci.* **1980**, *91*, 449.
- Maradudin, A. A.; Montroll, E. W.; Weiss, G. H.; Ipatova, I. P. *Theory of Lattice Dynamics in the Harmonic Approximation*; Academic Press: New York, 1971.
- Solid State Theory-Methods and Applications*; Landsberg, P. T., Ed.; Wiley-Interscience: London, 1969.
- Born, M.; Huang, K. *Dynamical Theory of Crystal Lattice*; Oxford U. P.: London and New York, 1954.
- Tsekov, R.; Ruckenstein, E. *J. Chem. Phys.* **1994**, *100*, 1450.

Width Operator for Resonance Width Determination

Tae Jun Park

Department of Chemistry, Dongguk University, Seoul 100-715, Korea

Received December 18, 1995

The resonance width may be directly determined by solving an eigenvalue equation for width operator which is derived in this work based on the method of complex scaling transformation. The width operator approach is advantageous to the conventional rotating coordinate method in twofold; 1) calculation can be done in real arithmetics and, 2) so-called θ -trajectory is not required for determining the resonance widths. Application to one- and two-dimensional model problems can be easily implemented.

Introduction

Resonance phenomena occur in various physico-chemical processes including electron-molecule scattering,¹ simple gas-phase reactions such as $\text{H} + \text{H}_2$.² Thus they play important roles in understanding chemical reactions from the dynamical viewpoint. In addition, attempts have been made to

relate resonance states with the transition state of chemical reactions.^{3,4} The resonance phenomena are generally described as the sharp variations of cross sections at certain energies E_R (resonant energies) and are related to the existence of nearly bound states.⁵

Theoretically resonance can be accurately determined as the pole of scattering matrix.⁵ Evaluation of the scattering